Journal of the European Ceramic Society 15 (1995) 135–143

0955-2219/95/$9.50

Surface Decontamination Treatments of Undoped $BaTiO_3$—Part I: Powder and Green Body Properties

Claude Hérard, Annelise Faivre & Jacques Lemaître*

École Polytechnique Fédérale de Lausanne (EPFL), Laboratoire de Technologie des Poudres, MX-Ecublens, CH-1015 Lausanne, Switzerland

(Received 3 March 1994; revised version received 17 June 1994; accepted 30 June 1994)

Abstract

Five commercial barium titanate powders were subjected to various surface decontamination treatments: calcination at 500°C, followed by leaching either in pure water or acetate buffer solution. They were then de-agglomerated by ultrasonic treatment and finally characterised by XRD, TGA, XPS, EGA, pyrolysis/FT-IR, BET specific surface area and particle size analysis. The main contaminating elements in raw powders were carbon and sulphur, present as barium carbonate (between 0·7 and 1·2wt%) and barium sulphate (about 0·5 wt%). Barium sulphate is thermally stable up to 1400°C and is not affected by the treatments. Barium carbonate decomposes in two steps, between 500 and 900°C and 1200 and 1400°C by reaction with TiO_2 and $BaTiO_3$ to release CO_2. Carbonation is slightly reduced by calcination, but subsequent water cleaning promotes re-carbonation. Acid cleaning substantially decreases the $BaCO_3$ content, down to 0·07–0·7 wt%. The remaining quantity corresponds to the most stable form which decomposes near 1200–1400°C and is still partially present at the surface of the particles. Forming of ceramics green bodies by slip casting of aqueous suspensions stabilised by ammonium poly(acrylate) was then investigated. The dispersing solution compositions have been optimised for each powder and treatment, in order to minimise the liquid/solid ratio of the slip. In all cases, the properties of the slips and of the cast specimens have been improved by the cleaning treatments: higher solid volume fractions in the slip up to 60% for the best case and higher green densities. In particular green densities as high as 70% have been obtained which is very close to the theoretical maximum packing density of log-normally polydispersed spheres. This enhancement can be ascribed to the beneficial effect of decarbonation on the de-agglomeration of the powders.

* To whom correspondence should be addressed.

1 Introduction

Over the past few years it has become evident that different commercial ceramic powders which are apparently identical according to supplier's data (in particular with respect to stoichiometry, granulometry, surface area and bulk composition) actually exhibit quite different behaviour during the processing steps to produce a final product. This variability is mainly related to the surface chemistry of the powders, which is very difficult to control during the elaboration process and is also very sensitive to handling (storage, contact with atmosphere). The surface of the particles can be contaminated with impurities, whose nature, amount and impact on subsequent processing is not completely understood.

Barium titanate, which is still the most widely used material in the electronic industry for capacitors[1] and positive temperature coefficient of resistivity (PTCR) devices,[2] is typically faced with these problems. Its surface is contaminated either with impurities present in the raw materials, or with carbonates,[3] which result from exposure to atmospheric CO_2 or are produced during the synthesis of the powders[4] (high-temperature solid state, wet chemical or hydrothermal). The presence of this impure surface layer can be detrimental to forming, in particular slip casting, because it alters the rheological properties of the slip,[5] either by enhancing frictional forces between surfaces of the particles, or by promoting the formation of agglomerates. The optimal solid volume fraction in the slip is consequently reduced and results in low green densities after drying. Also the sintering step is affected, with an increased porosity which eventually weakens the final properties (especially dielectric strength). Therefore, it would be interesting to be able to modify available commercial powders[6] by appropriate surface treatments in order to gain reproducibility from one powder

source to another and obtain the desired final ceramic properties.

The aim of this work presented in a series of two papers is to elucidate the exact influence of surface contamination in undoped barium titanate powders and investigate the possibility and consequences of its elimination. Therefore five commercial powders representative of different synthesis routes have been selected and subjected to various thermal and chemical treatments aimed at removing their surface carbonate. In Part I, decontamination treatments (calcination, cleaning in aqueous solution and in acid solution) are described. Investigation of the powders by X-ray diffraction (XRD), thermogravimetric analysis (TGA), X-ray photoelectron spectroscopy (XPS), evolved gas analysis (EGA), pyrolysis/infra-red spectroscopy (PY/FT-IR), specific surface area measurement and particle size distribution analysis are then reported. The effect of such treatments on casting green bodies from aqueous slips stabilised with ammonium poly(acrylate) is presented. Statistical design and analysis of experiments were used throughout this study, and results are discussed in terms of liquid limit of the slips and green densities. In Part II, the sintering behaviour of such surface modified powders will be described and correlated with relevant physical parameters of the initial powders.

2 Experimental procedure

Five commercial $BaTiO_3$ powders were used in this study: Criceram lot VPP20, TAM HPB lot 688, TAM HPB lot 745, Cabot BT10 lot 6243-24, and Rhône-Poulenc type Elmic BT 100 lot 7958. The three first powders were synthesised by the oxalate route, the fourth one by hydrothermal synthesis and the last one by suspending titania sols in barium nitrate aqueous solutions followed by drying, calcination and milling.[7] The supplier's main specifications are summarised in Table 1. Impurities such as Ca, Si, K, Cr, Fe, Sr, Na, Al are present in all powders, without exceeding 100 ppm, except Sr (<600 ppm).

Thermal treatment was intended to decompose surface barium carbonate and possible organic additives present in the raw powders. They were calcined at 500°C for 16 h in air. Since the treatment resulted in agglomeration of the powders, they were subjected to ultrasonic de-agglomeration just after calcination (see later).

Table 1. Suppliers' specifications of initial powders

Powder	*Ba/Ti*	*Specific surface area (m^2/g)*	*Median diameter by volume (μm)*
Criceram	0·99	2·5	1·3
Rhône-Poulenc	1·000	2·7	0·84
TAM 688	0·998	3·22	1·41
TAM 745	0·998	2·89	1·43
Cabot	1·007	7·87	0·4

Chemical treatment was performed on non de-agglomerated calcined powders in order to complete the surface decontamination treatment. 0·3M acetic acid–ammonium acetate buffer (pH of 4·5) was used: [CH_3COOH (50%) + CH_3COONH_4 (50%)]. 50g of each powder were put into 200 cm^3 of this cleaning solution. These amounts were determined from $BaCO_3$ content in raw powders, estimated from preliminary TGA measurements, and assuming the consumption of 20% of the acetic acid during the carbonate dissolution. The stirred suspensions (250 rpm) were maintained for 16 h at 30°C, the powders were then centrifuged, the supernatant was discarded and replaced by boiled demineralised water; washing was repeated until constant conductivity of the supernatant was obtained. The powders were then dried in a desicator in primary vacuum using $CaCl_2$ as a desiccant and finally ground lightly in an agate mortar. In order to ensure that the acid cleaning treatment has no secondary effects inherent to manipulations (suspension, drying), a control cleaning experiment with boiled demineralised water was performed under exactly the same conditions and used as a reference.

De-agglomeration of the powders in suspension by ultrasonic treatment was studied using a 2^4 factorial statistical design. The factors investigated were (A) sonication time (20–40 min), (B) volume of the suspension (125–250 cm^3), (C) solid weight fraction (20–40 wt%) and (D) nature of the solvent (either water or isopropanol). Optimal conditions were found to be 30 min ultrasonication with a 150W horn in boiled demineralised water (50 g of powder in 200 cm^3 water). After sedimentation, the supernatants were removed and the powders were dried in a 32% relative humidity desicator with $CaCl_2$.

XRD experiments were performed on a Siemens Kristalloflex 805 diffractometer with the Ni-filtered Cu K_α wavelength on 10 mg samples.

Thermogravimetric measurements were performed on a Setaram 92-16.18 thermobalance, under flowing oxygen atmosphere. For each run, approximately 200 mg of powder were accurately weighed in a platinum crucible, and the temperature was raised from ambient up to 1000°C at 10°C/min and then from 1000 to 1400°C at 5°C/min.

XPS analyses were made with a Perkin-Elmer Phi 5500 ESCA system spectrometer using the Mg K_α line (15 keV–350W). Several mg of powder

were placed for each run on an indium substrate. The signal curves were fitted using Gaussian peaks summation and Shirley baseline subtraction.[8]

Chemical analyses were carried out on a specific carbon + sulphur analyser from Leybold-Heraeus type CSA 2003. For each measurement 0·1 g of powder, mixed with melting agents (1 g Fe + 0·5 g W) to ensure complete decomposition, were placed in a crucible in an induction furnace with flowing oxygen. The evolved gases were first separated from H_2O and then analysed by infrared detectors specially calibrated for CO_2 and SO_2.

FT-IR analyses were conducted with a Mattson Instruments Inc. type Galaxy 4020 spectrophotometer coupled to a CDS1000 pyrolysis unit. Flash pyrolyses (heating rate: 5°C/ms then 20s at 700 or 1300°C) were done on 5 mg of powder for each run, with nitrogen as carrier gas. The measuring chamber was carefully purged before each run in order to avoid erroneous measurements due to the presence of residual atmospheric carbon dioxide.

Specific surface areas of powders were measured by N_2 adsorption according to the BET model with a Micromeritics type Gemini 2360 surface area analyser. 3 g of powder were used for each measurement.

Particle size distributions of powders were determined with a Horiba CAPA-700 cuvet photo centrifuge, using 10 mg of powder and an aqueous solution of poly(acrylic acid) (0·8 wt%) as dispersion liquid. Prior to measurement the suspensions were ultrasonicated (P = 300W, 7 litre bath) for 10 min. The reliability of the results was guaranteed by four repetitions of the same measurement.

Slip-cast specimens were prepared for each powder source and each treatment from aqueous $BaTiO_3$ suspensions stabilised with poly(acrylic acid)(PAA),[9] the acidity of the stabiliser being neutralised by NH_3. For each powder and treatment, the composition of the dispersion liquid has been optimised in two steps.[10] Firstly, the response of the liquid limit of the powders (LL, defined as the minimum liquid/solid ratio necessary to obtain a free flowing slurry, in cm^3/g) to variations in the PAA concentration ([PAA] = 0·3–0·5 %wt) and the neutralisation ratio ($[NH_3]$/[PAA] = 1·2–1·5) was investigated, using a 2^2 factorial statistical design; LL was experimentally measured by adding to 2 g of dry powder the dispersing solution by increments of 20 μlitre, with strong agitation between two additions, up to the liquid point. Second, LL was minimised for each powder and treatment by acting on the factor(s) found to have a significant effect. The effect of the slip composition (i.e. [PAA] around the optimum value for LL, and liquid/solid ratio in smaller or larger excess above LL) was investigated and optimised using the same statistical methodology. The liquid limit is a processing parameter directly related to the viscosity of the slip and is very sensitive to the degree of agglomeration of the powder. It is easily determined on small quantities of material and provides ready to use information for the casting process. The slips were then vibrated for 30 s at 30 Hz, ultrasonicated (P = 300W, 7 litre bath) for two min, and outgassed for 2 min under vacuum. The slips were cast in a silicon rubber mould, placed on a flat gypsum base; direct contact between the samples and the gypsum base was prevented by inserting a 0·2 μm cellulose membrane. Samples were prepared this way in the form of blocs (12·5 × 6·5 × 6·5 mm) for dilatometry measurements. The samples were withdrawn from the mould after 15 min and then left to dry for 24 h in a desicator containing $CaCl_2$ as a desiccant (32% relative humidity).

Green densities have been measured by Archimedes' method, using isopropanol as the immersion liquid, and assuming the value of 6·02 g/cm^3 for the theoretical density of $BaTiO_3$; the samples were first saturated with isopropanol under vacuum (0·15 bar).

3 Results

3.1 Powder properties

The presence of barium carbonate, which is thought to be the major contaminant at the surface of raw powders, has been investigated by *X-ray diffraction*. Only two crystalline phases were detected: tetragonal $BaTiO_3$ and orthorhombic $BaCO_3$. After acid cleaning the peaks corresponding to barium carbonate have disappeared, as shown in Fig. 1 for the Rhône-Poulenc powder.

Preliminary *thermogravimetric analyses* were performed in order to obtain quantitative data required for treatments of initial powders. Differential thermogravimetric curves of raw powders are shown in Fig. 2, and are similar for all

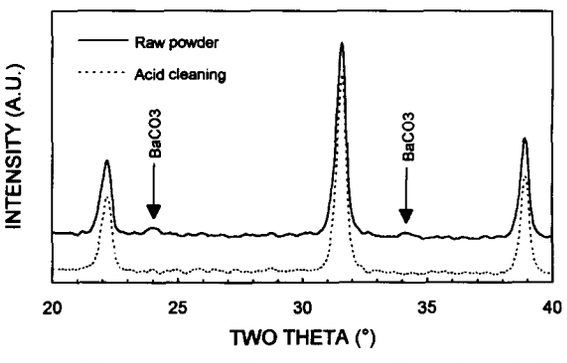

Fig. 1. XRD patterns for as-received and acid-cleaned Rhône-Poulenc powders.

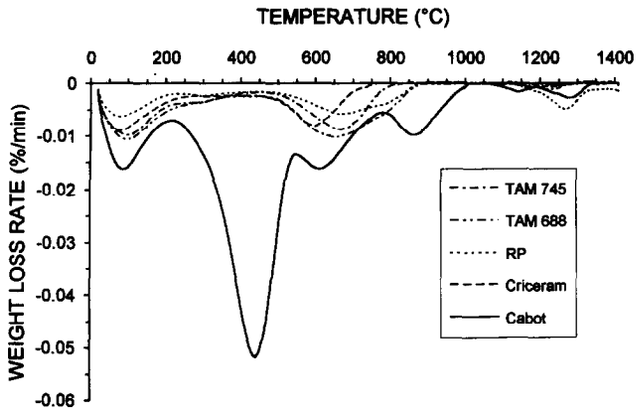

Fig. 2. DTG curves for as-received powders.

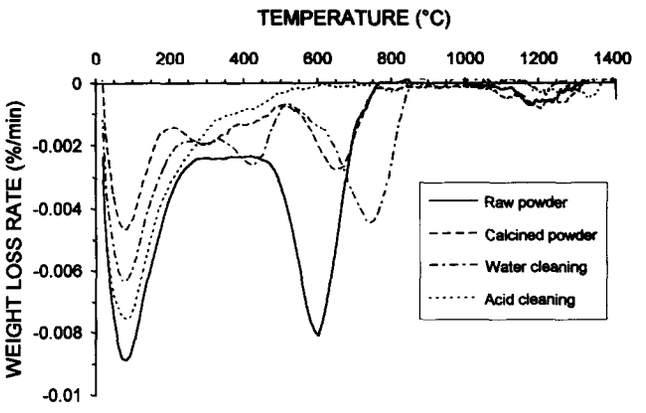

Fig. 4. DTG curves for Criceram powder.

powders: the first loss peak near 100°C results from adsorbed water removal. A second peak common to all powders between 500 and 900°C can be ascribed to the evolution of CO_2 upon $BaCO_3$ decomposition and represents 0·15–0·25% weight loss. Another diffuse peak common to all powders appears between 1200 and 1400°C: it represents only about 0·003 to 0·1 wt% and the nature of the corresponding gas release was ascertained with aid of other techniques (see later). The Cabot powder shows an extra broad peak between 200 and 600°C, due to the elimination of water incorporated in the perovskite lattice, which is typical of powders synthesised hydrothermally.[11]

The effect of the various treatments performed on the initial powders are clearly visible on DTG curves shown in Figs 3—7. In every case, calcination decreases only slightly the CO_2 losses between 500 and 900°C. Water cleaning following calcination has a negative effect with respect to $BaCO_3$ removal in that CO_2 losses increase again. Acid cleaning proves to be efficient for all powders, in that it totally eliminates the $BaCO_3$ loss peak between 500 and 900°C. The position of this peak remains unchanged after calcination and water cleaning for Cabot powder, while it is shifted to high temperatures are calcination then once again are water cleaning for the other powders. The diffuse loss peak above 1200°C is not significantly affected by the treatments, except for the Rhône-Poulenc powder, which exhibits an increase in weight loss in that temperature range after water and acid cleaning.

X-Ray photoelectron spectroscopy allowed the detection of only four elements at the surface of raw and treated powders: Ba, Ti, O and C. The ratio Ba/(Ba+Ti) calculated from the $Ba_{3d5/2}$ and Ti_{2p} transitions appears to decrease from 40 at.% for raw powders to 30 at.% after acid cleaning, meaning that Ba^{2+} ions have been dissolved and removed during this treatment. The shape of oxygen and carbon lines were not investigated in detail, because of their high sensitivity to the atmospheric contamination. The Ti_{2p} line consisted in every instance of a single narrow Gaussian peak, meaning that titanium is present only in a single chemical state, i.e. $BaTiO_3$. The $Ba_{3d5/2}$ transition could be resolved into two Gaussian components separated by 1·58 ± 0·09eV. The lower binding energy corresponds to the titanate environment, and the higher one can be ascribed to a carbonate environment.[12] After acid cleaning, this last peak is decreased by a factor of two when compared to the raw powder data, as shown in Fig. 8 for the Rhône-Poulenc powder. The fact that the peak

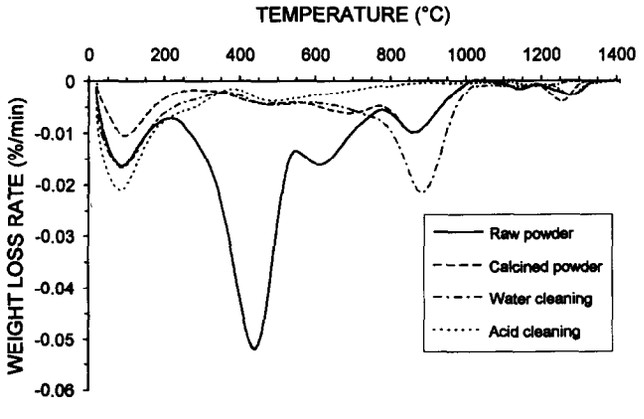

Fig. 3. DTG curves for Cabot powder.

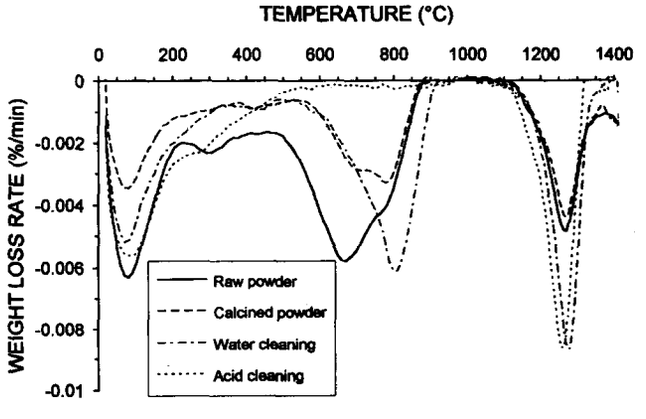

Fig. 5. DTG curves for Rhône-Poulenc powder.

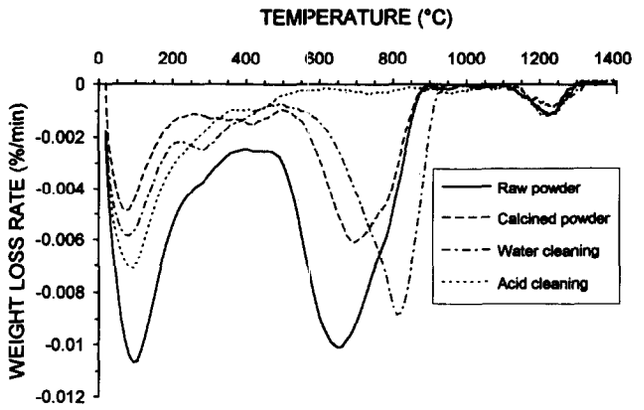

Fig. 6. DTG curves for TAM 688 powder.

has not completely disappeared after acid washing indicates that some $BaCO_3$ subsists at the surface of the particles.

Presence of elemental carbon and sulphur (which is a common contaminant in inorganic raw materials) has been investigated by *EGA* on Rhône-Poulenc calcined and acid-cleaned powders. It turns out that carbon (0·055wt%) and sulphur (0·067wt%) are both present in calcined powders, and that acid cleaning leaves the sulphur content unchanged and lowers the carbon content to 0·034wt%.

Gases released between 500 and 900°C and near 1300°C were identified on as-received powders by *FT-IR* analysis of evolving gas from a pyrolysis unit. FT-IR spectra obtained both at 600 and 1300°C on the same powder samples only reveal the presence of CO_2, as shown in Fig. 9.

Examination by *scanning electron microscopy (SEM)* of untreated, calcined water and acid-cleaned powders does not show any difference in surface roughness, nor in shape. The surface appears smooth in both cases, as shown in Fig. 10 for Rhône-Poulenc powder.

Specific areas of different powders before and after treatments are not affected by the treatments. Measured values are: 2·92 m^2/g for TAM 745 powder, 3·05 m^2/g for TAM 688 powder, 2·49 m^2/g for Rhône-Poulenc powder, 3·05 m^2/g for

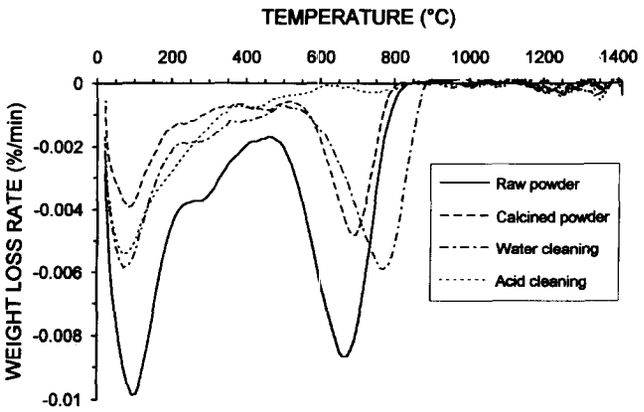

Fig. 7. DTG curves for TAM 745 powder.

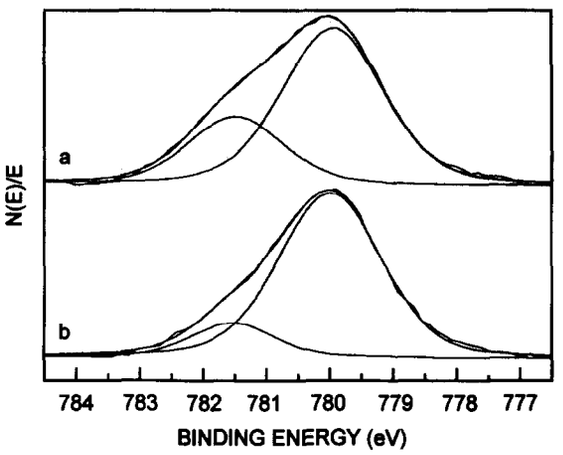

Fig. 8. $Ba_{3d5/2}$ XPS curve fit for Rhône-Poulenc powder. (a) As-received; (b) acid cleaned.

Criceram powder, and 7·79 m^2/g for Cabot powder. These values are in close agreement with the suppliers' data and confirm that the treatments have no influence on surface roughness.

Particle size distributions were determined for all powders and treatments, and are reasonably close to log-normal distributions. Calcination alone tends to slightly agglomerate the powders, which are then efficiently de-agglomerated by ultrasonication. Acid cleaning without ultrasonic de-agglomeration proved to de-agglomerate the calcined powders to the same extent as sonication alone, and subsequent ultrasonic treatment of acid-cleaned powders did not provide further improvement. Water cleaning alone did not show any significant effect. Figure 11 shows the effect of calcination–sonication and acid cleaning on Rhône-Poulenc powder particle size distribution (average of four runs): both treatments promote the removal of some agglomerates. The mean particle size remains unchanged.

3.2 Rheological properties

For all the powders, only [PAA] has been found to affect the *liquid limit* very significantly (above

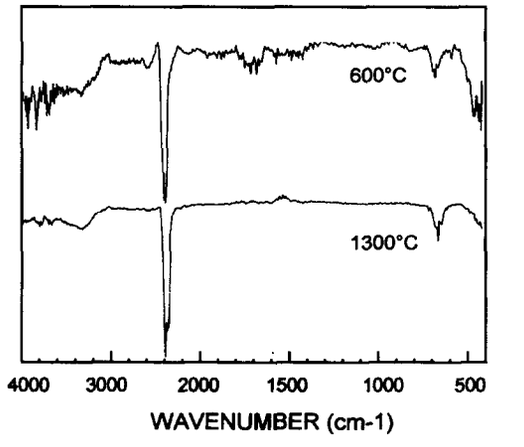

Fig. 9. Transmittance infrared spectra of gas evolved from pyrolysed Cabot raw powder at 600 and 1300°C.

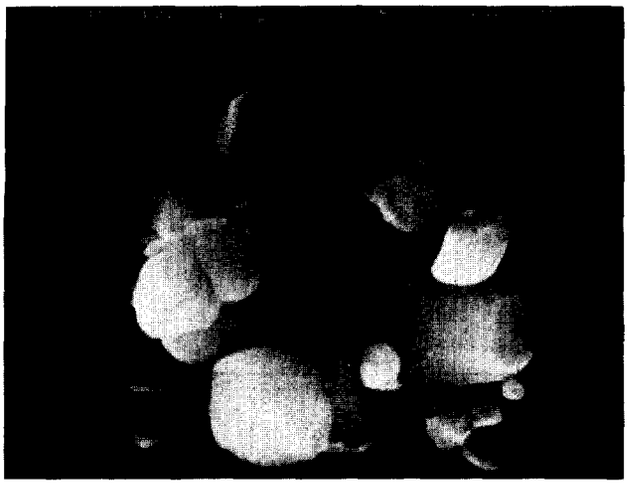

Fig. 10. SEM micrography of Rhône-Poulenc powder.

the 99·9% confidence level); within the experimental range investigated [NH_3]/[PAA] played no role, nor did it change the effect of [PAA]. The optimisation was thus conducted by varying [PAA] (0·10–1·00%wt), while keeping [NH_3]/[PAA] constant at 1·5. The effect of [PAA] on the liquid limit of raw powders is shown in Fig. 12. The lowest value for the liquid limit is reached for [PAA] = 0·6wt% for Criceram, TAM688, TAM745 and Rhône-Poulenc powders for all treatments, and between 0·8 and 1 %wt for Cabot powder depending on the treatments. The higher [PAA] level necessary for the Cabot powder is a consequence of its higher specific surface area. The corresponding optimal LL and [PAA] values are shown in Fig. 13. All the treatments have a positive effect by decreasing the liquid limit, the best improvement being for Cabot powder (−35% by acid cleaning). The best absolute value for LL is obtained for TAM 688 and Rhône-Poulenc powders after acid treatment, corresponding to a solid volume fraction in the slip higher than 60%. Acid-cleaning treatment is the most efficient in that sense except for Criceram powder, whose lowest LL is obtained on only calcined and sonicated powder. It has been observed that ultrasonic de-agglomeration of acid-cleaned powders does not improve the liquid limit.

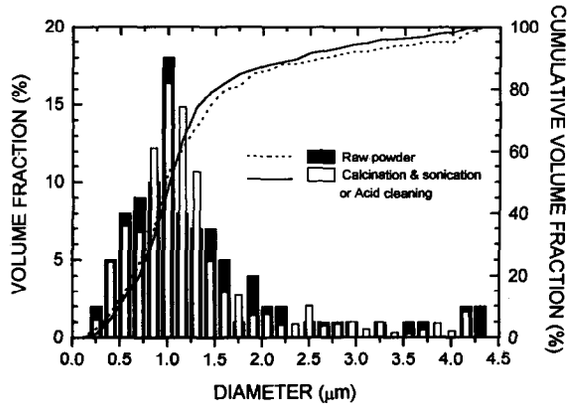

Fig. 11. Effects of treatments on particle size distribution.

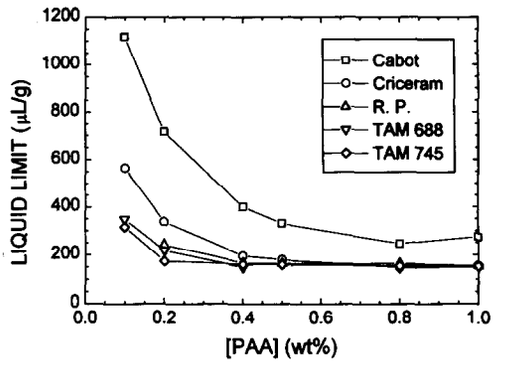

Fig. 12. [PAA] dependence of the liquid limit for raw powders ([NH_3]/[PAA] = 1·5).

3.3 Green body properties

The slip composition was then optimised in order to obtain the highest *green density*, by varying [PAA] (0·60–0·80 %wt) and the volume of dispersant added (LL + 0·025–0·050 cm^3/g). The slightly higher amount of dispersant with respect to LL is intended to compensate for evaporation during slip processing. Statistical analysis revealed a significant effect of the volume of dispersant, its lower level yielding the highest green densities for the five powders. Figure 14 shows the effect of the treatments on the green densities of cast samples, resulting from the average of four samples for each powder and treatment obtained with optimised slip compositions. Cabot raw specimens were too brittle to be manipulated and have not been considered for further studies. Large variations in relative green density can be seen with respect to the powder sources, between 57 and 70% theoretical density. Statistical analysis reveals that calcination and sonication treatment has drastically improved the green density, the most dramatic enhancement being for Rhône-Poulenc powder (+16%). However, acid or water cleaning do not significantly provide further improvement, confirming that de-agglomeration by acid cleaning is equivalent to sonication.

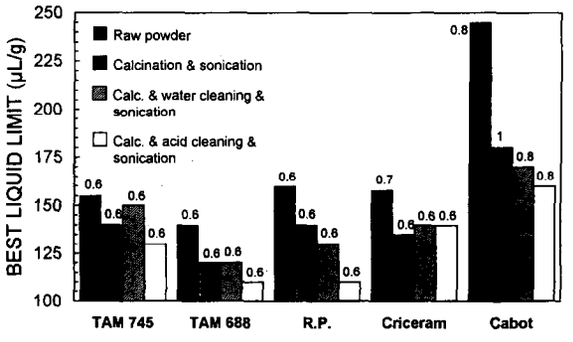

Fig. 13. Effects of treatments on the optimal liquid limit with corresponding [PAA] (in wt%).

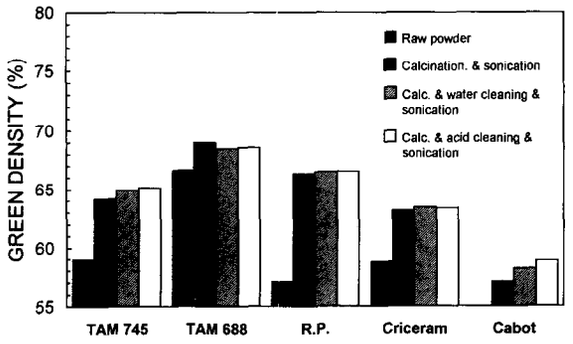

Fig. 14. Effects of treatments on green density.

4 Discussion

The major elemental contaminants in raw powders appear to be carbon and sulphur, in approximately the same weight concentration. XRD and XPS experiments show that carbon is present at the surface as barium carbonate. On the other hand, no sulphur compound was detected, neither by XRD, nor by XPS, suggesting that sulphur is distributed in the bulk of the particles, probably as $BaSO_4$, as a result of the preparation conditions of the $BaTiO_3$ powders.

FT-IR pyrolyses show that only CO_2 is released up to 1300°C; the absence of SO_2 or SO_3 release means that barium sulphate remains stable in that temperature range. The possibility of O_2 release (not detectable by infrared spectroscopy), by an exchange mechanism of oxygen between the $BaTiO_3$ lattice and the ambient atmosphere,[13] although reported for donor-doped $BaTiO_3$,[14] is not expected for undoped $BaTiO_3$ sintered in an oxidising atmosphere; TGA experiments performed in nitrogen still gave rise to similar weight losses, indicating that the origin of the gas release is not the atmosphere but the powders themselves. Therefore, weight losses observed by TGA on raw powders between 500 and 900°C, and 1200 and 1400°C, can definitely be ascribed to evolving CO_2.

Based upon this finding, three decomposition reactions for the barium carbonate contamination can be considered:[15]

$$BaCO_3 + TiO_2 \rightarrow BaTiO_3 + CO_2(g) \qquad T_d = 400{\cdot}5°C \quad (1)$$

$$BaCO_3 + BaTiO_3 \rightarrow Ba_2TiO_4 + CO_2(g) \qquad T_d = 1002°C \quad (2)$$

$$BaCO_3 \rightarrow BaO + CO_2(g) \quad T_d = 1540°C \quad (3)$$

where the decomposition temperatures T_d are computed using standard thermodynamic data[16] and assuming $p_{CO_2} = 1$ atm. Barium carbonate decomposes directly into barium oxide and carbon dioxide (reaction (3)) at a temperature higher than conventional sintering temperature for $BaTiO_3$.

Table 2. $BaCO_3$ content: Comparison of EGA and TGA estimations (Rhône-Poulenc powder)

Treatment	*Total [$BaCO_3$] (wt%) from EGA*	*Total [$BaCO_3$] (wt%) from TGA*	*Relative deviation (%)*
Calcined	0·910	0·942	3·4
Acid cleaned	0·551	0·718	23·2

The presence of $BaTiO_3$ or TiO_2 lowers its decomposition temperature; TiO_2 does not exists as a true second phase in the particles, but a compositional gradient $Ba_{1-x}TiO_{3-x}$ develops at the vicinity of the $BaCO_3/BaTiO_3$ interface. This results in a gas release in the sintering temperature range which is detrimental for obtaining high densities (see Part II).

Weight losses near 600 and 1300°C recorded on raw powders by TGA can thus be accounted for by reactions (1) and (2), respectively, the shift in temperature arising from the arbitrary value of 1 atm for p_{CO_2}. $BaCO_3$ content for all powders and treatments was then calculated from weight losses between 500 and 1400°C. Comparison with EGA measurement for Rhône-Poulenc powder showed relatively good agreement, as shown in Table 2.

For all treatments the barium sulphate content remains unchanged, due to its high decomposition temperature, low solubility and distribution in the bulk of the particles. Figure 15 shows the total barium carbonate content present for all powders and treatments, based on TGA measurements. Raw powder carbonation is not correlated with particle size; it is probably determined by a combination of synthesis conditions and ageing phenomena.

Examination of DTG curves of Figs 4, 5, 6 and 7 shows that for Criceram, Rhône-Poulenc, TAM 688 and TAM 745 powders, the calcination treatment promotes the dissociation of the most reactive part of the carbonate (low-temperature side of the 600°C loss peak), with a corresponding shift towards higher temperature of the resultant maximum loss rate. This easily decomposable carbon-

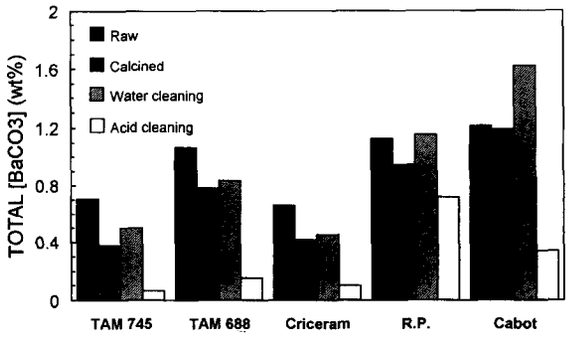

Fig. 15. Effects of treatments on total $BaCO_3$ content.

ate probably arises from atmospheric contamination. After water cleaning the 600°C loss peak is increased again, meaning that recarbonation due to CO_2 dissolved in water has occurred. This $BaCO_3$ species formed in aqueous conditions is more stable because it decomposes at a slightly higher temperature (850°C instead of 650°C). In contrast, the corresponding loss peak for Cabot powder (Fig. 3) is not affected by calcination and water-cleaning treatments, and is also centred on 850°C: The $BaCO_3$ contaminating the surface originates from the hydrothermal synthesis, resists calcination at 500°C and has the same features that those formed during water cleaning.

A substantial amount of carbonate is eliminated by acid cleaning. Recarbonation of acid washed powders does not take place because the surface is deficient in barium due to Ba^{2+} ions going into solution. TGA experiments performed six months after the treatment do not show any recarbonation.

On the other hand, $BaCO_3$ is not completely eliminated by acid cleaning (weight losses above 1100°C). Two consecutive acid cleaning treatments using the same acetate buffer (0·3M) were then performed in order to try to dissolve the remaining carbonate, but without any improvement. This suggests that barium carbonate contamination originates from different mechanisms: surface alteration, by contact with atmosphere or water, producing carbonate decomposing at low temperature (TG losses between 500 and 900°C) and easily removed by acid cleaning, and contamination during the synthesis of the powders (incomplete reactions, contaminated precursors, etc.), resulting in a more stable form of carbonate decomposing at higher temperature (TG losses between 1100 and 1400°C). This phase is still partially present at the surface after acid cleaning, as shown by XPS. Its low solubility in the cleaning solution is probably because it is more tightly bonded to the $BaTiO_3$ surface. Free carbonate grains are not likely to resist acid-cleaning treatment, but the possibility of a bulk contamination of the particles, i.e. $BaCO_3$ entrapped in $BaTiO_3$ crystals, could also be consistent with the partial removal upon acid cleaning.

The effects of the various treatments on forming can be summarised as follows: For all powders, calcination alone tends to agglomerate the powders; calcination in association with the ultrasonic de-agglomeration treatment promotes a higher green density. The same improvement results after acid cleaning of calcined powders without subsequent sonication, and a further ultrasonic treatment of acid-cleaned powders does not improve the green density, showing the efficient de-agglomerating effect of acid washing. The liquid limit of the slips is also markedly improved after calcination and sonication, and acid cleaning brings about a further improvement. Compared to calcination, water cleaning does not change significantly the green density and the liquid limit, which means that modifications by acid cleaning are definitely not due to handling artefacts (suspending, de-agglomeration and drying).

Physical characteristics of individual particles of $BaTiO_3$ such as morphology, diameter and specific surface area do not seem to be affected by the decontamination treatments. The surface carbonate distribution, either homogeneous or heterogeneous, cannot be inferred from SEM analysis, because the carbonate layer thickness is below the resolution of the apparatus. XPS analysis shows that $BaCO_3$ still subsists at the surface after acid cleaning, so that the colloidal stabilisation mechanisms involved in the slips elaboration are almost unaffected (cf. PAA content in Fig. 13). It can be concluded that the improvements of the liquid limits of the slips (i.e. decrease in viscosity) by the treatments result mainly from their de-agglomerating effects. Acid cleaning does not always improve the green density and the liquid limit to the same extent. However, a lower green density can be compensated by a larger shrinkage during drying.

The improvement due to cleaning treatments, as far as rheological and green body properties are concerned, can be interpreted according to the following scheme. In raw powders, some $BaTiO_3$ particles form soft agglomerates, $BaCO_3$ acting as a 'cement'. Calcination treatment, by its temporary decomposition of $BaCO_3$, may be sufficient to destroy these soft agglomerates. Acid cleaning is a more drastic treatment: not only does it dissolve $BaCO_3$, but it can also slightly alter the $BaTiO_3$ surface and in some instances totally dissolve the necks between partially sintered particles that form hard agglomerates (chemical de-agglomeration). The improvement of green body properties already reported can then be accounted for by a geometric argument: the surface treatments performed appear to decrease the number of agglomerates present in raw powders and consequently increase the packing efficiency by minimising bridging effects between particles. The highest green density value of 70%, obtained with calcined TAM 688 powder, is remarkably close to the theoretical maximal packing density of about 72% predicted from computer simulation[17,18] for random close packing of log-normally distributed spheres with a geometric standard deviation of 1·7, as measured for this powder.

5 Conclusions

The study presented in the first part of this series of two papers shows that commercial undoped $BaTiO_3$ powders are mainly contaminated by barium sulphate and barium carbonate. Barium sulphate is thermally stable beyond 1400°C and is unaffected by heat or washing treatments. Barium carbonate, on the other hand, thermally decomposes in two steps, near 600°C and 1300°C, to release CO_2. This carbonation originates from two sources: atmospheric or aqueous CO_2 contamination results in the formation of a surface $BaCO_3$ layer, easily decomposed, either thermally or chemically. Carbonate originating from the synthesis stage is more stable, resists acid cleaning and decomposes above 1200°C. It is thought that carbonate remaining after acid cleaning is mainly distributed at the surface of the particles, without excluding a residual bulk contamination. The decarbonating effect of the calcination or chemical treatments (acid dissolution), although not complete, proved to be substantially beneficial with respect to green body densities of ceramics samples obtained by slip casting. For all powders the liquid limits of the slips have been decreased and the green density increased, respectively as much as 35% and 16%. Advantage may be taken of the corresponding reduction of shrinkage during sintering for obtaining complex shape samples. These improvements can be seen as a consequence of the elimination of agglomerates present in raw powders, as a result of the reduction of surface barium carbonate content yielding figures very close to the theoretical optimal values of packing density. A point to note is that the range within which the processing parameters vary as a function of powder source has been substantially reduced by the treatments, which means that a better reproducibility of ceramic green samples can be achieved by controlling the surface chemistry of the raw powders.

Acknowledgements

The Swiss National Foundation is gratefully acknowledged for financial support. The authors are grateful to Dr Y. Houst for EGA measurements, to Mr N. Xanthopoulos for XPS measurements, to M. R. Mullone for SEM analysis and Dr P. Bowen for his assistance in the preparation of the manuscript.

References

1. Chiou, B. S., Lin, S. T., Duh, J. G. & Chang, P. H., Equivalent circuit model in grain boundary barrier layer capacitors. *J. Am. Ceram. Soc.*, **72**(10) (1989) 1967-75.
2. Fagan, J. G. & Amarakoon, V. R. W., Reliability and reproducibility of ceramic sensors: Part II, PTC thermistors. *Am. Ceram. Soc. Bull.*, **72**(2) (1993) 69–76.
3. Kingery, W. D., Bowen, H. K. & Uhlmann, D. R., *Introduction to Ceramics*. John Wiley and Sons, NY, 1976.
4. Jaffe, B., Cook, Jr, W. R. & Jaffe, H., *Piezoelectric Ceramics*. Academic Press, London and NY, 1971.
5. Dobias, B., *Coagulation and Flocculation. Theory and Applications*. Marcel Dekker, NY, 1993.
6. Fernandez, J. F., Duran, P. & Moure, C., Influence of surface modification on sintering of $BaTiO_3$. In *Proceedings of the 2nd European Ceramic Society Conference*, Vol. 3, ed. G. Ziegler & H. Hausner. Deutsche Keramische Gesellschaft e.V., Augsburg, 1991, pp. 1891–5.
7. Lavielle, D., Poumarat, J., Montardi, Y., Bernard, P. & Aguerre-Charriol, O., Microstructure/properties relationships in chemically processed barium titanate for X7R characteristics. In *Proceedings of the 2nd European Ceramic Society Conference*. Vol. 3, ed. G. Ziegler & H. Hausner. Deutsche Keramische Gesellschaft e.V., Augsburg, 1991, pp. 1903–7.
8. Briggs, D. & Seah, M. P., *Practical surface analysis*, 2nd edn, Vol. 1, *Auger and X-Ray Photoelectron Spectroscopy*. John Wiley & Sons, Chichester, 1990.
9. Chen, Z. C., Ring, T. A. & Lemaître, J., Stabilization and processing of aqueous $BaTiO_3$ suspension with polyacrylic acid. *J. Am. Ceram. Soc.*, **75**(12) (1992) 3201–8.
10. Lemaître, J., Hérard, C. & Vogel, D., Microstructure and piezoelectric properties of slip cast barium titanate ceramics. In *Proceedings of the 3rd European Ceramic Society Conference*, Vol. 2, ed. P. Duran & J. F. Fernandez. Faenza Editrice Iberica, Madrid, 1993, pp. 59–64.
11. Hennings, D. & Schreinemacher, S., Characterization of hydrothermal barium titanate. *J. Eur. Ceram. Soc.*, **9** (1992) 41–6.
12. Hung, C. C., Riman, R. E. & Caracciolo, R., An XPS investigation of hydrothermal and commercial barium titanate powders. In *Ceramic Powder Science III*, Vol. 12, ed. G. L. Messing, S. Hirano & H. Hausner. The American Ceramic Society, Inc., Westerville, 1990, pp. 17–25.
13. Chan, N. H., Sharma, R. K., & Smyth, D. M., Nonstoichiometry in undoped $BaTiO_3$. *J. Am. Ceram. Soc.*, **64**(9) (1981) 556–62.
14. Drofenik M., Popovic, A., Irmancnik, L., Kolar, D. & Krasevec, V., Release of oxygen during the sintering of doped $BaTiO_3$ ceramics. *J. Am. Ceram. Soc.*, **65**(12) (1982) C203–4.
15. Beauger, A., Mutin, J. C. & Niepce, J. C., Synthesis reaction of metatitanate $BaTiO_3$. Part I. Effect of the gaseous atmosphere upon the thermal evolution of the system $BaCO_3$—TiO_2. *J. Mat. Sci.*, **18** (1983) 3041–6.
16. Barin, I. & Knacke, O., *Thermochemical Properties of Inorganic Substances*. Springer, Berlin, 1973.
17. Nolan, G. T. & Kavanagh, P. E., Computer simulation of random packings of spheres with log-normal distributions. *Powder Technology*, **76** (1993) 309–16.
18. Yu, A. B. & Standish, N., An analytical-parametric theory of the random packing of particles. *Powder Technology*, **55** (1988) 171–86.